Turkish Journal of Electrical Engineering & Computer Sciences

http://journals.tubitak.gov.tr/elektrik/

Research Article

Turk J Elec Eng & Comp Sci
(2013) 21: 2127 – 2140

doi:10.3906/elk-1201-41

ANFIS-based estimation of PV module equivalent parameters: application to a stand-alone PV system with MPPT controller

Ahmet Afşin KULAKSIZ*
Department of Electrical and Electronics Engineering, Faculty of Engineering, Selçuk University, Konya, Turkey

Received: 15.01.2012 • **Accepted:** 04.07.2012 • **Published Online:** 30.10.2013 • **Printed:** 25.11.2013

Abstract: The performance and system cost of photovoltaic (PV) systems can be improved by employing high-efficiency power conditioners with maximum power point tracking (MPPT) methods. Fast implementation and accurate operation of MPPT controllers can be realized by modeling the characteristics of PV modules, obtaining equivalent parameters. In this study, adaptive neuro-fuzzy inference systems (ANFISs) have been used to obtain 3 of the parameters in a single-diode model of PV cells, namely series resistance, shunt resistance, and diode ideality factor. The input parameters of ANFISs are a material-type of PV modules, short circuit current, open circuit voltage, and unit area under the I-V curve of the PV module. The advantage of the proposed method is that the equivalent parameters can be obtained for a wide range of PV modules of different types (monocrystalline, multicrystalline, and thin-film) using easily obtainable electrical parameters. To demonstrate the accuracy of the proposed model, MPPT control is implemented in a PV system with a battery charge application for 3 different types of PV modules. The obtained results suggest that the ANFIS model appears to be a useful tool for estimating the equivalent parameters of PV modules.

Key words: ANFIS, single diode model, equivalent circuit parameter, maximum power point tracking, PV system

1. Introduction

Photovoltaic (PV) sources are being used more and more in many applications, including battery charging, home powering, satellite power systems, water pumping applications, and communication systems. One way to improve the system cost and effective operation of PV systems is to employ maximum power point tracking (MPPT) methods in high-efficiency power conditioners. The MPPT method is used to maximize the PV array output power, irrespective of the environmental conditions and the load electrical characteristics.

Various MPPT methods have been addressed in the literature, including open-circuit voltage, short-circuit current, incremental conductance, and perturbation and observation (P&O) methods [1,2]. Open-circuit voltage and short-circuit current methods assume that the voltage at the maximum power point (V_{mpp}) and current (I_{mpp}) is proportional to the open circuit voltage and short-circuit current, respectively. However, the estimated values are only an approximation of the true values, and they also change with the aging of the PV modules. The P&O method is the most commonly used one, due to its ease of implementation. The operating principle of the P&O and incremental conductance methods are a perturbing duty cycle and observing the power output, which provides the information for obtaining the new duty cycle. It was reported that both methods did not perform well during the rapid changing of atmospheric conditions [3].

*Correspondence: afsin@selcuk.edu.tr

Because of the fact that PV systems can be considered as nonlinear, artificial intelligence methods, namely artificial neural networks (ANNs), fuzzy sets, and genetic algorithms can be effectively applied on PV energy systems for increased system performance. The artificial intelligence methods have recently found application in fields such as PV system sizing, MPPT control, and the optimal configuration of PV systems. Most of the applications employed a feed-forward multilayer perceptron (MLP) neural network or radial basis function network (RBFN) structure for modeling the PV modules and the MPPT operation of PV systems [4–8]. ANN-based controllers have been used to estimate the voltages and currents corresponding to the maximum power point of PV modules for variable temperature and solar radiation. However, the accurate modeling of PV modules requires a large number of training data consisting of a wide range of environmental conditions. Moreover, the obtained model is unique for a particular type and brand of PV module, and the off-line implementation of an ANN-model requires powerful microcontrollers. The main contribution of this work is that the equivalent parameters can be extracted for a wide range of PV modules of different types using a small number of parameters that can be easily obtained from field tests.

In the literature, several methods, such as the iterative method [9], fuzzy logic [10], ANN [7,8,11,12], and evolutionary algorithms [13,14], have been employed for determining the model parameters of the PV modules. One way for the fast implementation and accurate operation of MPPT controllers is to model the characteristics of the PV modules, obtaining equivalent parameters. In this study, adaptive neuro-fuzzy inference systems (ANFISs) have been used to obtain 3 of the parameters in the single-diode model of the PV cells, namely the series resistance, shunt resistance, and diode ideality factor. Therefore, solving any nonlinear implicit equations, as in the conventional methods, is not necessary. The input parameters of the ANFIS are a material-type of the PV modules, short circuit current, open circuit voltage, and unit area under the I-V curve of the PV module. The advantage of the proposed method is that the equivalent parameters can be obtained for a wide range of PV modules of different types (monocrystalline, multicrystalline, and thin-film) using easily obtainable electrical parameters. The advantage of the proposed method is that the time-consuming, laborious process of the training process, as well as the off-line implementation of the ANFIS, is implemented by employing the current tremendous processing power of PCs, and the results can be used to create a model of PV modules. Therefore, very complex and costly microcontrollers or digital signal processors are not needed for the off-line implementation of ANFISs. The obtained model is used to demonstrate the MPPT capability of the proposed method in a PV system with a battery charge application. The simulation results of the implemented MPPT method with a low calculation burden are introduced.

The paper is organized as follows. The theoretical background related to the solar cells and ANFIS is reviewed in Section 2. The proposed method is explained in Section 3. The results from the implemented ANFIS models and the MPPT capability of a stand-alone PV system for a battery charging application is presented and discussed in Section 4. The final conclusions are addressed in Section 5.

2. Theoretical background

2.1. Solar cell characteristics

The basic element of a PV system is the solar cell. A typical solar cell consists of a p-n junction that is formed in a semiconductor material similar to a diode. As shown in Figure 1, the equivalent circuit model of a solar cell consists of a current generator, I_L, and a diode plus series R_s and parallel R_{sh} resistance [15]. The series and parallel combination of solar cells form solar PV arrays rated at the required output voltage and current. Once the I-V characteristics of a single solar cell are determined, the model is expanded to determine the behavior of a PV array or module.

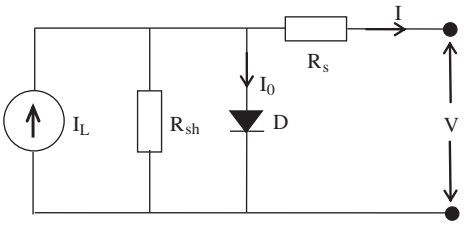

Figure 1. The equivalent circuit of a solar cell.

The current-voltage characteristic of a single cell is described by the Shockley solar cell equation [15]:

$$I = I_L - I_0 \left[\exp\left(\frac{V + I.R_s}{n.V_{th}} \right) - 1 \right] - \frac{V + I.R_s}{R_{sh}}, \tag{1}$$

where I is the output current, I_L is the generated current under a given insolation, I_0 is the diode reverse saturation current, n is the ideality factor for a p-n junction, R_s is the series loss resistance, and R_{sh} is the shunt loss resistance. V_{th} is known as the thermal voltage. For an individual cell, it is calculated from:

$$V_{th} = k.T/q, \tag{2}$$

where k is the Botzmann constant (1.3806×10^{-23} J/K), T is the cell temperature (in Kelvin), and q is the electron charge (1.6022×10^{-19} C).

The saturation current, I_0, of the solar array varies with temperature according to the following equation:

$$I_0 = I_r \left[\frac{T}{T_r} \right]^3 \exp\left[\frac{qE_{GO}}{n.k} \left(\frac{1}{T_r} - \frac{1}{T} \right) \right], \tag{3}$$

where T_r is the reference temperature, I_r is the saturation current at T_r, and E_{GO} is the band-gap energy of the semiconductor used in the solar array. In Eq. (1), I_L is a function of the incident solar radiation and cell temperature, and is given by:

$$I_L = \left[I_{scr} + K_I (T - T_r) \right] \frac{G}{100}, \tag{4}$$

where I_{scr} is the short circuit current at reference temperature T_r, K_I is the short circuit current temperature coefficient, and G is the insolation in mW/cm^2.

Eqs. (1) to (4) clearly demonstrate that 5 parameters need to be calculated to characterize the equivalent circuit shown in Figure 1. The short circuit current, open circuit voltage, and maximum power voltages and currents are substituted in Eq. (1) to obtain 3 equations that allow for expressing some parameters in terms of the other ones. Several researchers used polynomial approximate equations using experimentally obtained coefficients to obtain these parameters. However, the iterative processes are very sensitive to the initial values. Therefore, obtaining a good solution may depend on the selected initial values [16,17].

If the short circuit, open circuit, and maximum power voltage and current values are substituted in Eq. (1), 3 equations are obtained to express some parameters in terms of the other ones. For the short-circuit conditions, after some minor simplifications, I_L can be expressed by [16]:

$$I_L \approx \frac{I_{sc}.(R_s + R_{sh})}{R_{sh}}. \tag{5}$$

Similarly, for the open-circuit conditions, taking into account the result of Eq. (5), and after a small approximation, I_0 can be expressed by [16]:

$$I_0 \approx \frac{I_{sc}.(R_s + R_{sh}) - V_{OC}}{R_{sh}} . \exp\left(-\frac{V_{OC}}{n.V_{th}}\right). \tag{6}$$

Substituting the voltage and current values for the maximum power point in Eq. (1) and substituting Eq. (5) gives another equation for I_0 [16]:

$$I_0 = \left[\frac{(I_{SC} - I_{MP}).(R_s + R_{sh}) - V_{MP}}{R_{sh}}\right] . \exp\left(-\frac{V_{MP} + I_{MP}.R_s}{n.V_{th}}\right). \tag{7}$$

According to Eqs. (5)–(7), in a single-diode model of PV cells, the I_L and I_0 parameters can be expressed by n, R_s, and R_{sh} [16]. Therefore, in this study, 3 equivalent circuit parameters are estimated by an artificial intelligence-based approach, and the I_L and I_0 parameters can be readily computed using Eqs. (5) and (7), which was explained by the procedure presented in [16].

As the analytical and mathematical approach of the problem results in a cumbersome procedure, an artificial intelligence-based approach is a viable option as a function approximation problem [10–14], and the ANFIS can be used to estimate these 3 equivalent circuit parameters. A MPPT controller can be implemented based on this model.

2.2. Adaptive neuro-fuzzy inference systems

Combining the advantages of neural networks, such as having a black-box model, and the linguistic interpretability of a fuzzy inference system (FIS), ANFISs can be applied to many complicated problems [18]. For a fuzzy inference system, with 2 inputs and 1 output, a common rule set with 2 fuzzy if-then rules is shown by Eq. (8) for a first-order Sugeno fuzzy model.

$$\begin{array}{l} \text{Rule 1: If } x\text{is } A_1 \text{ and } y \text{ is } B_1, \text{ then } f_1 = p_1 x + q_1 y + r_1, \\ \text{Rule 2: If } x \text{ is } A_2 \text{ and } y \text{ is } B_2, \text{ then } f_2 = p_2 x + q_2 y + r_2. \end{array} \tag{8}$$

As shown in Figure 2, the ANFIS architecture for the Sugeno fuzzy model includes 5 layers, in which nodes of the same layer have similar functions.

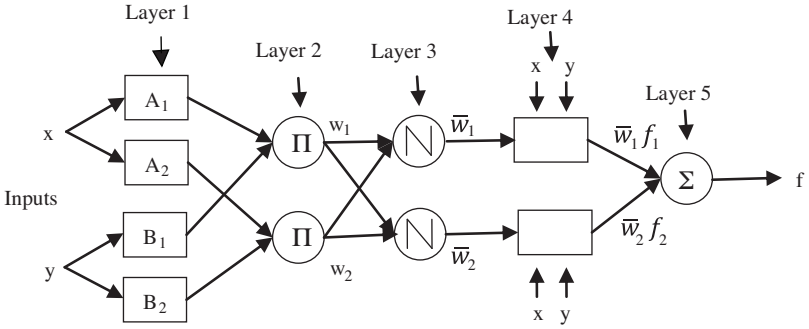

Figure 2. ANFIS architecture of a 2-input first-order Sugeno fuzzy model with 2 rules.

In Layer 1, every node i is an adaptive node with a node function:

$$\begin{array}{lll} O_{1,i} = \mu_{A_i}(x), & \text{for} & i = 1, 2, \\ O_{1,i} = \mu_{B_{i-2}}(y), & \text{for} & i = 3, 4, \end{array} \tag{9}$$

where x (or y) is the input to node i and A_i (or Bi-2) is a linguistic label associated with this node. Here, the membership function for A can be any appropriate parameterized membership function. Parameters in this layer are referred to as premise parameters [18].

Every node in Layer 2 is a fixed node labeled Π, whose output is the product of all of the incoming signals:

$$O_{2,i} = w_i = \mu_{A_i}(x)\mu_{B_i}(y), i = 1, 2. \tag{10}$$

Each node output represents the firing strength of a rule. In Layer 2, any other T-norm operators that perform fuzzy AND can be used as the node function.

Every node in Layer 3 is a fixed node labeled N. The ith node calculates the ratio of the ith rule's firing strength to the sum of all rules' firing strengths:

$$O_{3,i} = \bar{w}_i = \frac{w_i}{w_1 + w_2} i = 1, 2. \tag{11}$$

Every node in Layer 4 is an adaptive node with a node function:

$$O_{4,i} = \bar{w}_i f_i = \bar{w}_i(p_i x + q_i y + r_i), \tag{12}$$

where $\bar{w}_i$ is a normalized firing strength from Layer 3 and $\{p_i, q_i, r_i\}$ is the parameter set of this node, which are referred to as consequent parameters.

The single node in Layer 5 is a fixed node labeled Σ that computes the overall output as the summation of all of the incoming signals:

$$\text{overall output} = \mathrm{O}_{5,i} = \sum_i \bar{w}_i f_i = \frac{\sum_i w_i f_i}{\sum_i w_i}. \tag{13}$$

The constructed adaptive network is functionally equivalent to a Sugeno fuzzy model. In this adaptive network, Layers 3 and 4 can be combined to obtain an equivalent network with only 4 layers.

It is demonstrated that when the number of rules is not restricted, a zero-order Sugeno model has an unlimited approximation power for matching any nonlinear function arbitrarily well. As a universal approximator, the ANFIS is a viable alternative to be employed for obtaining the equivalent circuit parameters of PV modules.

3. ANFIS approach to PV module modeling and MPPT operation

For modeling the PV modules, the information provided by the manufacturers is usually insufficient. The modeling can be done in an easy way by making an a priori estimation of any parameter [19]. In many cases, the ideality factor is assigned a value and the resistance values are obtained from this [20]. These methods usually offer results with great uncertainty [16]. In the literature, for better accuracy for modeling the PV modules, the most widely accepted method is to use a large number of experimental data [21,22]. The current studies in this field have focused on methods with reduced data for accurately modeling the PV modules. As an example, the authors in [16] require as the input data only the open circuit voltage, the short circuit current, and the maximum power point voltage and current. The main objective of our study is to obtain accurate results by including the manufacturing type and the unit area under the I-V curve of the PV module to the input data. In this study, the ANFIS architecture programmed in MATLAB is used to develop a model for the

PV modules to be employed in the MPPT operation of the PV systems [23]. Therefore, solving any nonlinear implicit equations necessary in conventional methods is not required here.

In this study, the Takagi–Sugeno-type fuzzy system, which yields crisp values rather than a linguistic variable, has been employed. The network model has 4 inputs, namely the material type, open circuit voltage, short circuit current, and a value obtained from the I-V curve of the PV module. This value is calculated from the ratio of the area under the I-V curve to the multiplication of I_{sc} and V_{oc}. The area between the I-V curve and x-axis is calculated by the definite integral and a value between 0 and 1 is calculated in regard to the shape of the I-V curve, which is mostly dependent on the equivalent circuit parameters, such as R_s and R_{sh}. These values for the area under the I-V curve are calculated for each PV module brand using the Sandia National Laboratory characteristic model developed by Sandia National Laboratory [24,25].

In this study, it is proposed that together with the manufacturing type, short circuit current, and open circuit voltage, the unit area of the I-V curve can be a good estimation tool to obtain the equivalent parameters, namely R_s, R_{sh}, and n. For the 3 outputs, 3 different ANFIS structures are created. The developed structure for each ANFIS used for modeling the PV modules is shown in Figure 3 [23].

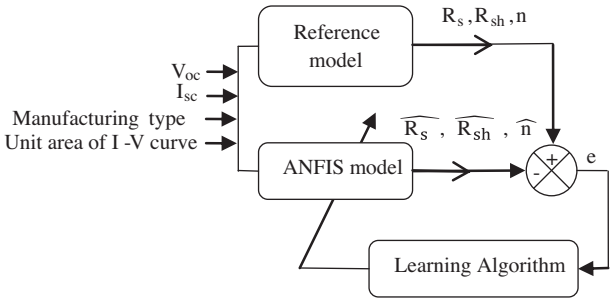

Figure 3. Proposed ANFIS models for predicting the equivalent electrical circuit parameters.

A set of 400 data pairs is used for training the developed ANFIS model. Three different PV module manufacturing types, namely monocrystalline, multicrystalline, and thin film, are present in the dataset and the created model is particularly effective for these manufacturing types of PV modules.

A set of 30 data samples that is not included in the training is used for the testing. The stopping criterion is completing 10 training epochs. As ANFIS converges very fast, there is no need to use more than 10 training epochs. The weights are batch-updated and a bell-shaped curve is used as a membership function (MF). Each MF takes 3 parameters stored in the weight vector of the bell fuzzy axon and the output of the fuzzy axon is computed by:

$$MF(x,w) = \frac{1}{1+\left|\frac{x-w_2}{w_0}\right|^{2w_1}}, \tag{14}$$

where x represents the input and w represents the weight of the bell fuzzy axon. The MFs of fuzzy axons can be modified through back propagation during training to accelerate convergence.

4. Results and discussion

4.1. Implementation of ANFIS models

A total of 400 data pairs are used for training. In each ANFIS structure, the number of fuzzy rules is chosen as 5. The learning algorithm is a hybrid combining back propagation, gradient-descent, and a least-squares algorithm.

After training, completely unknown data parameters are presented to the model and the performance is tested. Figure 4 shows the comparisons of the actual and simulated values for checking the data set. The accuracies of the obtained models for PV modules are analyzed through a comparison between checking the data provided from the manufacturer and the corresponding simulated data obtained from the ANFIS output. Figures 4a, 4b, and 4c show the analysis results for each ANFIS structure created to extract the ideality factor (n), series resistance (R_s), and shunt resistance (R_{sh}), respectively. The average testing error obtained for n is 0.0373, for R_s is 0.004116, and for R_{sh} is 24.911.

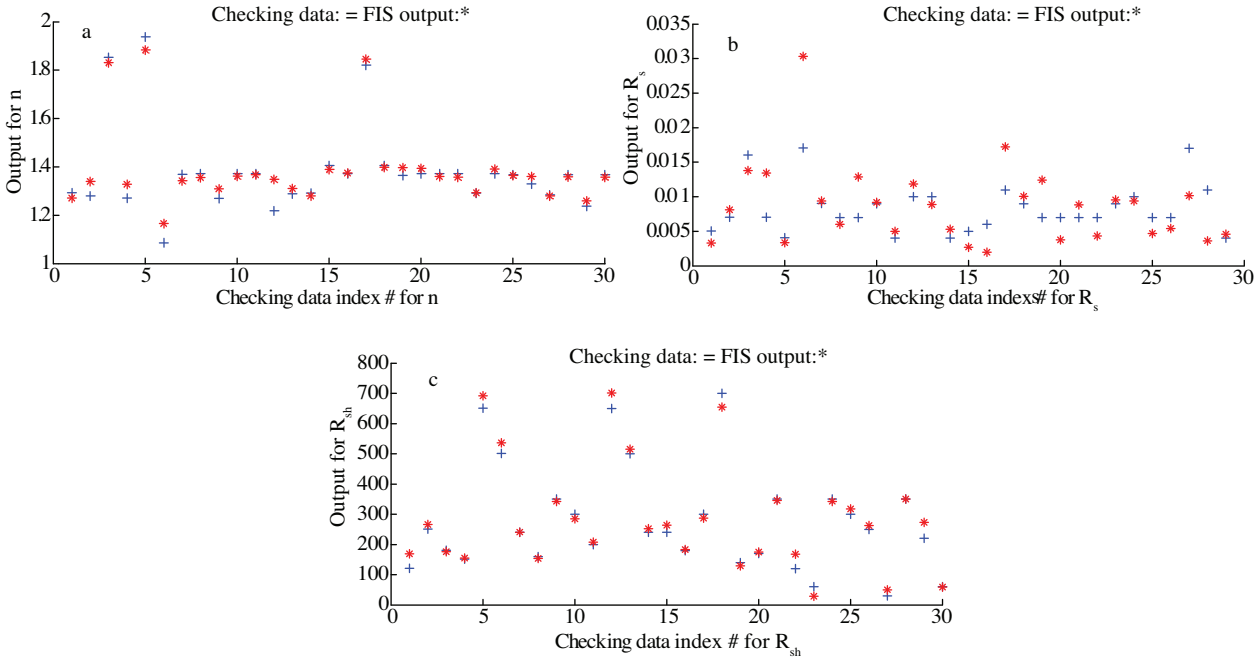

Figure 4. Comparison of the actual data (checking data) and ANFIS extracted data (FIS output) for the equivalent parameters of the PV modules, namely a) n, b) R_s, and c) R_{sh}.

Table 1 shows the actual equivalent parameters provided from the manufacturer and the predicted parameters of n, R_s, and R_{sh} obtained by means of the ANFIS for 3 different types of PV modules, namely monocrystalline (Shell SP70 [26]), polycrystalline (Kyocera KC60 [27] and Shell S75 [28]), and thin film (Shell ST40 [29]). The electrical characteristic data for these PV modules at standard test conditions (STC) are given in Table 2. The predicted values are obtained from testing the proposed ANFIS models for each equivalent parameter. The I_L and I_0 values are determined from Eqs. (5) and (7), and consequently, the single-diode equivalent circuit can be built. In Table 1, the P_{max} values are estimated at a solar irradiance of 600 W/m^2 and at 25 °C. It can be seen from Table 1 that the proposed ANFIS-based model shows good correspondence to the actual data, and therefore this model can be considered sufficient for the purpose of further study.

Figures 5a and 5b show the relative percentage errors for the V_{mp} and I_{mp} values at different irradiance levels and at a 25 °C constant temperature for the utilized PV modules, namely Shell SP70 (monocrystalline), Kyocera KC60, Shell S75 (multicrystalline), and ST40 (thin-film). The practical data from the manufacturers of PV modules are used in the percentage relative error calculation as actual data. The temperature is kept constant at 25 °C. The relative error is the difference of the actual and proposed method results of the V_{mp} and I_{mp} values divided by the actual values.

Table 1. Estimated equivalent parameters of 3 different kinds of PV modules.

	Shell SP70		Kyocera KC60		Shell S75		Shell ST40	
	monocrystalline		multicrystalline		multicrystalline		thin film	
	Actual	Predicted	Actual	Predicted	Actual	Predicted	Actual	Predicted
	value	value	value	value	value	value	value	value
R_s (Ω)	0.44	0.47	0.15	0.17	0.19	0.17	1.14	1.17
R_{sh} (Ω)	180	204	450	413	200	173	300	318
N	1.3	1.28	1.35	1.37	1.35	1.36	1.5	1.48
P_{max}	41.6	41.72	34.05	34.83	43.63	43.47	23.74	23.87

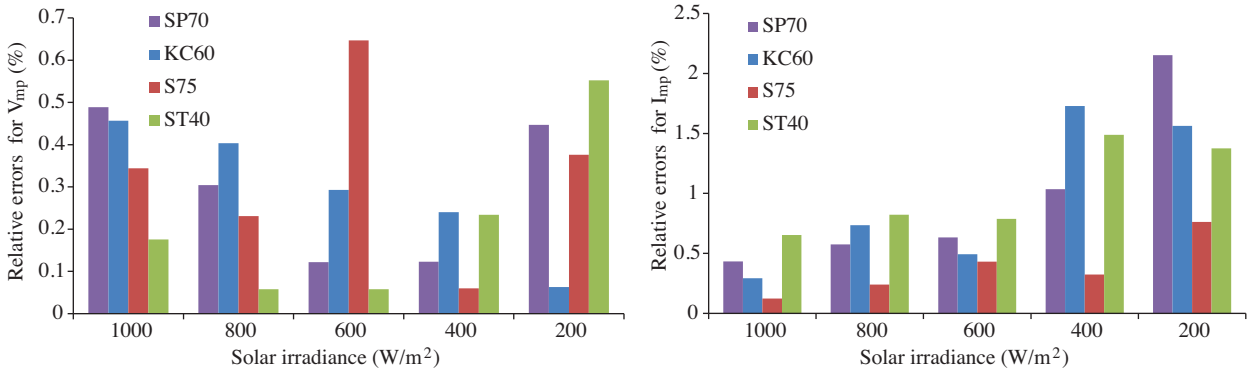

Figure 5. Percentage relative error values for a) V_{mp} and b) I_{mp}, calculated at different solar irradiance values for different kinds of solar modules.

A high precision on the output voltage and current at the maximum power points of PV modules can be obtained by creating a model of PV modules using the ANFIS. From Figures 5a and 5b it can be seen that when the PV voltage or PV current is used as a reference to operate the MPPT controller, for moderate and high solar irradiance values, the relative errors lie below 1%. Figure 5a implies that using the PV voltage as a reference may guarantee an error below 1% in the MPPT operation. Another major advantage of the proposed model is that it is effective for different silicon technologies as the training data include 3 different manufacturing types. As the obtained model is simple, the MPPT operation can be easily implemented using low-cost microcontrollers.

Table 2. Electrical characteristic data for the employed PV modules at STC.

Model	Maximum power (W)	Maximum power voltage (V)	Maximum power current (A)	Open circuit voltage (V)	Short circuit current (A)	Number of cells per module	Cell technology
Shell SP70	70	16.5	4.25	21.4	4.7	36	Monocrystalline
Kyocera KC60	60	16.9	3.55	21.5	3.73	36	Polycrystalline
Shell S75	75	17.6	4.26	21.6	4.7	36	Polycrystalline
Shell ST40	40	16.6	2.41	23.3	2.68	42	CIS/thin-film

To validate the model, the values have been analyzed at 4 important points in the I-V curves for 4 PV modules with different technologies. Tables 3–6 show the relative errors for V_{oc}, I_{sc}, V_{mp}, and I_{mp}, obtained at different solar irradiances. The tables present the calculated values by the Sandia model [24], and the simulation results implemented in the MATLAB environment using Eqs. (1)–(7), with the actual equivalent parameter

values provided from the manufacturer and the simulation results for the equivalent parameters obtained by the ANFIS models proposed in this paper. The temperature was kept constant at 25 °C. As can be seen in these tables, the proposed model generates satisfactory results for a wide range of operating conditions. Unlike the previous works suggested by other researchers, an iterative technique is not required, and the proposed method is more advantageous compared with the conventional nonlinear programming techniques [30,31]. Because the method does not depend on the initial conditions, trapping to local minima solutions can be avoided.

4.2. Application to a stand-alone PV system with battery charging

To evaluate further the performance of the proposed PV model in the MPPT operation, a PV system with a battery charging application has been simulated. The model-based MPPT algorithm is implemented in a DC-DC converter to maximize the power generated by the PV module, independently of the temperature and solar irradiation. The schematic diagram of the PV system implemented in the power electronics simulator (PSIM) simulation software [32] is shown in Figure 6. Here, in order to simulate the PV modules and implement the MPPT algorithm, the codes are built in Visual C++ software and linked to the simulation by dynamic link libraries. In the PVMODEL.dll module, a single-diode model of the PV modules has been built to simulate the different kinds of PV modules investigated in this paper. The MPPT.dll module is used as a controller to implement the MPPT algorithm, including the proportional-integral–type control. The inputs into the controller are the solar irradiance (G), temperature (T), PV voltage (V_{PV}), and PV current (I_{PV}), and the single output is used to produce the reference signal for the DC-DC buck converter. The MPPT operation in the circuit is implemented based on the voltage. In the proposed method, the maximum power points for the corresponding solar irradiance and temperature values are searched by solving the obtained equations for the single-diode model of PV modules.

The PV system is tested for 3 kinds of PV modules under changing insolation conditions. The results for the theoretical and proposed method are shown in Figures 7a–7d. The actual parameters and the parameters from the proposed method are used to model the PV modules in the PSIM schematic, at a constant temperature of 25 °C, and for a step change of the solar irradiation between 800 and 1000 W/m^2.

The results demonstrate that the acquired model is sufficiently accurate for real-time MPPT applications. Compared with the conventional P&O algorithm, the model-based algorithm provides a better transient response, as the MPP is obtained beforehand and a search is not required. The method also performs well for rapidly changing atmospheric conditions, as the calculations can be done very fast and the MPP is tracked using the obtained reference value. Because the obtained model is simple, the MPPT operation can be easily implemented using low-cost microcontrollers.

The proposed ANFIS-based estimation method can be applied to the widely available manufacturing type of PV modules present on the market. This advantage is provided by the reason that the training data include 3 different types.

For higher accuracy of the results and to increase the generalization ability, a larger amount of training data should be provided to the ANFIS. It should be noted that, for the newer technology of PV modules, the predictive performance can be satisfactory only if the training data are provided to characterize the new technology of PV modules. Otherwise, accurate results are not guaranteed for new samples outside of the available training set.

Table 3. Predicted PV array characteristic parameters for the Sandia model, simulation results using the actual equivalent parameters, and the ANFIS-based model for the Shell SP70 monocrystalline PV module for different irradiation intensities at 25 °C.

Irradiation	Sandia model results				Simulation results				ANFIS-based results			
intensity (W/m^2)	V_{oc}(V)	I_{sc}(A)	V_{mp}(V)	I_{mp}(A)	V_{oc}(V)	I_{sc} (A)	V_{mp}(V)	I_{mp}(A)	V_{oc}(V)	I_{sc}(A)	V_{mp}(V)	I_{mp}(A)
1000	21.4	4.70	16.5	4.24	21.37	4.68	16.37	4.25	21.38	4.69	16.29	4.27
800	21.17	3.76	16.56	3.42	21.1	3.75	16.43	3.39	21.11	3.75	16.38	3.41
600	20.85	2.82	16.55	2.57	20.74	2.81	16.41	2.53	20.76	2.81	16.39	2.54
400	20.29	1.87	16.35	1.72	20.23	1.87	16.24	1.66	20.26	1.87	16.26	1.67
200	19.49	0.94	15.87	0.87	19.32	0.93	15.66	0.79	19.37	0.94	15.73	0.81

Table 4. Predicted PV array characteristic parameters for the Sandia model, simulation results using the actual equivalent parameters, and the ANFIS-based mode for the Kyocera KC60 multicrystalline PV module for different irradiation intensities at 25 °C.

Irradiation	Sandia model results				Simulation results				ANFIS-based results			
intensity (W/m^2)	V_{oc}(V)	I_{sc}(A)	V_{mp}(V)	I_{mp}(A)	V_{oc}(V)	I_{sc}(A)	V_{mp}(V)	I_{mp}(A)	V_{oc}(V)	I_{sc}(A)	V_{mp}(V)	I_{mp}(A)
1000	21.50	3.73	16.90	3.55	21.43	3.72	17.52	3.42	21.44	3.73	17.24	3.46
800	21.21	2.98	16.90	2.83	21.15	2.98	17.34	2.72	21.15	2.99	17.27	2.74
600	20.85	2.23	16.84	2.12	20.78	2.23	17.07	2.03	20.78	2.22	17.02	2.05
400	20.33	1.49	16.62	1.41	20.25	1.49	16.65	1.33	20.25	1.49	16.73	1.35
200	19.46	0.74	15.85	0.70	19.33	0.74	15.82	0.64	19.33	0.74	15.81	0.66

Table 5. Predicted I-V array characteristic parameters for the Sandia model, simulation results using the actual equivalent parameters, and the ANFIS-based model for the Shell S75 multicrystalline PV module for different irradiation intensities at 25 °C.

Irradiation	Sandia model results				Simulation results				ANFIS-based results			
intensity (W/m^2)	V_{oc}(V)	I_{sc}(A)	V_{mp}(V)	I_{mp}(A)	V_{oc}(V)	I_{sc}(A)	V_{mp}(V)	I_{mp}(A)	V_{oc}(V)	I_{sc}(A)	V_{mp}(V)	I_{mp}(A)
1000	21.63	4.80	17.6	4.34	21.64	4.69	17.45	4.29	21.63	4.69	17.51	4.28
800	21.96	3.82	18.23	3.46	21.35	3.75	17.32	3.42	21.34	3.75	17.36	3.41
600	20.91	2.88	17.48	2.59	20.98	2.81	17.11	2.55	20.97	2.81	17.12	2.54
400	20.34	1.91	16.48	1.64	20.45	1.87	16.74	1.67	20.43	1.88	16.73	1.62
200	19.56	0.96	16.56	0.86	19.52	0.93	15.95	0.80	19.48	0.94	15.89	0.82

Table 6. Predicted I-V array characteristic parameters for the Sandia model, simulation results using the actual equivalent parameters, an the ANFIS-based model for the Shell ST40 thin-film PV module fordifferent irradiation intensities at 25 °C.

Irradiation	Sandia model results				Simulation results				ANFIS-based results			
intensity (W/m^2)	V_{oc}(V)	I_{sc}(A)	V_{mp}(V)	I_{mp}(A)	V_{oc}(V)	I_{sc}(A)	V_{mp}(V)	I_{mp}(A)	V_{oc}(V)	I_{sc}(A)	V_{mp}(V)	I_{mp}(A)
1000	22.20	2.59	16.60	2.41	23.22	2.65	17.10	2.33	23.23	2.66	17.07	2.34
800	21.75	2.11	16.34	1.95	22.89	2.12	17.24	1.85	22.90	2.13	17.23	1.86
600	21.29	1.59	16.08	1.46	22.46	1.59	17.28	1.37	22.48	1.59	17.29	1.38
400	20.52	1.06	15.55	0.97	21.83	1.06	17.11	0.88	21.86	1.06	17.15	0.89
200	19.2	0.53	14.44	0.48	20.66	0.53	16.30	0.40	20.72	0.53	16.39	0.40

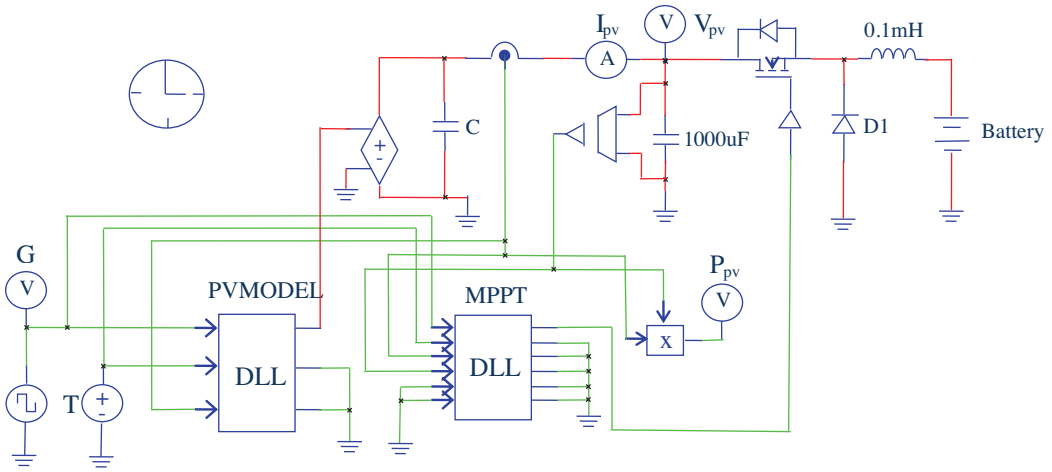

Figure 6. Schematic diagram of the PV system with a battery charging application.

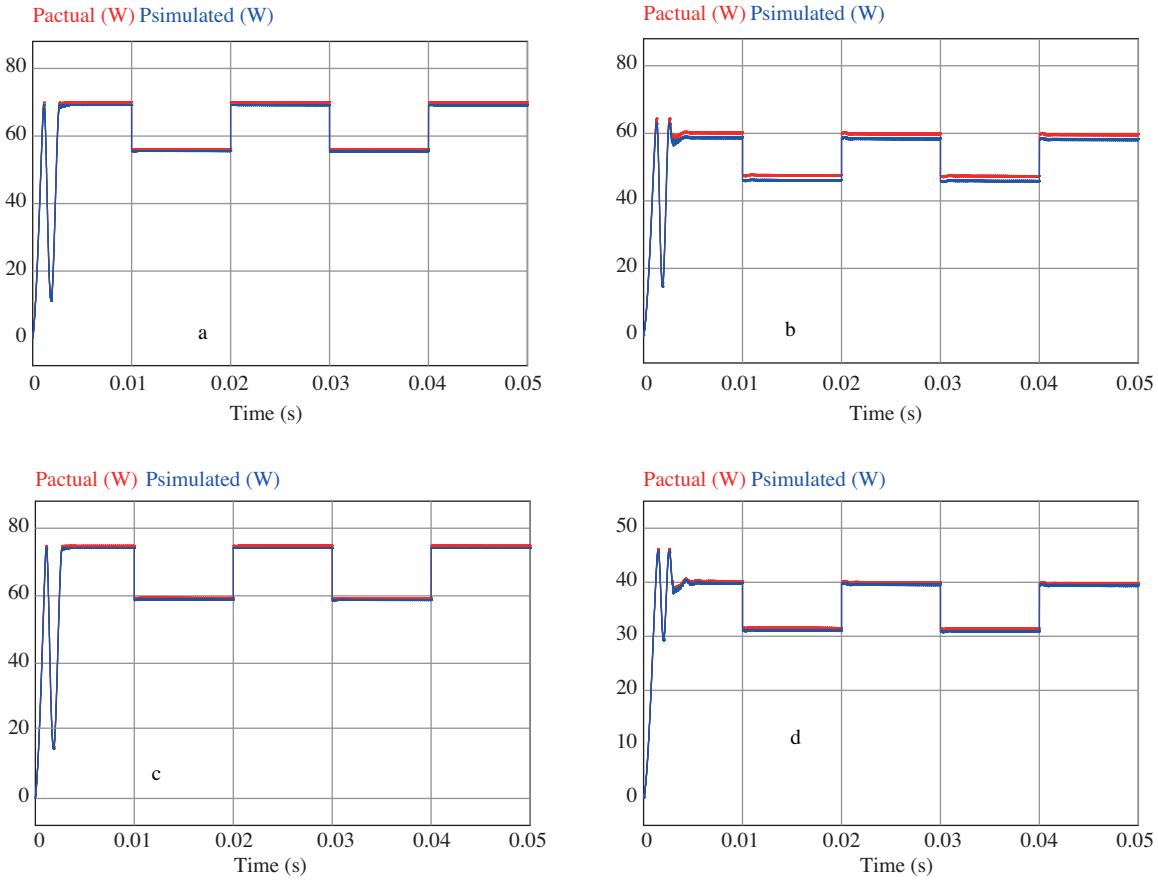

Figure 7. Power curves from the actual and proposed methods, obtained from the simulated PV system for changing solar irradiation values between 800 and 1000 W/m^2 for a) Shell SP70, b) Kyocera KC60, c) Shell S75, and d) Shell ST40.

5. Conclusion

The equivalent circuit parameters of the PV modules were obtained based on the ANFIS to characterize the circuit model of a real PV module. The ANFIS was employed as a dependable and robust method to build a nonlinear relationship and mapping between the easily obtainable experimental data and the equivalent parameters of the PV modules. Therefore, solving any nonlinear implicit equations, as in conventional methods, was not necessary. Three types of PV modules were used to evaluate the effectiveness of the modeling method and the parameters were found to be accurate enough to characterize the PV module. An advantage of the proposed method was that it does not rely on manufacturing data and experimental measurements can be used for parameter extraction. Therefore, manufacturing tolerances do not corrupt the results, and parameter extraction is implemented based on the PV module under study. Moreover, the variations depending on the aging effects on PV module parameters eventually were not omitted by the proposed method.

The model was successfully employed in a PV system with a power converter and controller. The MPPT accuracies were found to be in close agreement with the theoretical prediction. The major advantage of the proposed method is that the artificial intelligence-based model is not unique for one brand of PV module, but different manufacturing types of PV modules can be characterized. It was proven from the results that the developed model can be used to implement the MPPT controller as software embedded in a cost-effective microcontroller with low processing power. The proposed method can also be a useful tool for PV system designers for the optimal configuration of a PV system.

Acknowledgment

The author would like to express gratitude to the Selçuk University Scientific Research Support Fund (B.A.P.) for their financial support.

References

[1] V. Salas, E. Olias, A. Barrado, A. Lazaro, "Review of the maximum power point tracking algorithms for stand-alone photovoltaic systems", Solar Energy Materials and Solar Cells, Vol. 90, pp. 1555–1578, 2006.

[2] T. Esram, P.L. Chapman, "Comparison of photovoltaic array maximum power point tracking techniques", IEEE Transactions on Energy Conversion, Vol. 22, pp. 439–449, 2007.

[3] C.C. Chu, C.L. Chen, "Robust maximum power point tracking method for photovoltaic cells: a sliding mode control approach", Solar Energy, Vol. 83, pp. 1370–1378, 2009.

[4] M. Veerachary, T. Senjyu, K. Uezato, "Neural-network-based maximum-power-point tracking of coupled inductor interleaved-boost-converter-supplied PV system using fuzzy controller", IEEE Transactions on Industrial Electronics, Vol. 50, pp. 749–758, 2003.

[5] A.K. Rai, N.D. Kaushika, B. Singh, N. Agarwal, "Simulation model of ANN based maximum power point tracking controller for solar PV system", Solar Energy Materials and Solar Cells, Vol. 95, pp. 773–778, 2011.

[6] A.A. Kulaksız, R. Akkaya, "Training data optimization for ANNs using genetic algorithms to enhance MPPT efficiency of a stand-alone PV system", Turkish Journal of Electrical Engineering & Computer Sciences, Vol. 20, pp. 241–254, 2012.

[7] A. Al-Amoudi, L. Zhang, "Application of radial basis function networks for solar-array modeling and maximum power-point prediction", IEE Proceedings on Generation, Transmission and Distribution, Vol. 147, pp. 310–316, 2000.

[8] L. Zhang, Y.F Bai, "Genetic algorithm-trained radial basis function neural networks for modeling photovoltaic panels", Engineering Applications of Artificial Intelligence, Vol. 18, pp. 833–844, 2005.

[9] M.G. Villalva, J.R. Gazoli, E.R. Filho, "Comprehensive approach to modeling and simulation of photovoltaic arrays", IEEE Transactions on Power Electronics, Vol. 24, pp. 1198–1208, 2009.

[10] T.F. Elshatter, M.T. Elhagree, M.E. Aboueldahab, A.A. Elkousry, "Fuzzy Modeling and Simulation of Photovoltaic", 14th European Photovoltaic Solar Energy Conference, 1997.

[11] E. Karatepe, M. Boztepe, M. Çolak, "Neural network based solar cell model", Energy Conversion and Management, Vol. 47, pp. 1159–1178, 2006.

[12] F. Almonacid, C. Rus, L. Hontoria, M. Fuentes, G. Nofuentes, "Characterisation of Si-crystalline PV modules by artificial neural networks. Renewable Energy", Vol. 34, pp. 941–949, 2009.

[13] N. Moldovan, R. Picos, E. Garcia-Moreno, "Parameter extraction of a solar cell compact model using genetic algorithms", Spanish Conference on Electron Devices, pp. 379–382, 2009.

[14] K. Ishaque, Z. Salam, An improved modeling method to determine the model parameters of photovoltaic (PV) modules using differential evolution (DE). Solar Energy, Vol. 85, pp. 2349–2359, 2011.

[15] E. Lorenzo, Solar Electricity Engineering of Photovoltaic Systems, Artes Graficas Gala, S.L., Madrid, Spain, 1994.

[16] C. Carrero, D. Ramírez, J. Rodríguez, C.A. Platero, "Accurate and fast convergence method for parameter estimation of PV generators based on three main points of the I–V curve", Renewable Energy, Vol. 36, pp. 2972–2977, 2011.

[17] M.A. De Blas, J.L. Torres, E. Prieto, A. García, "Selecting a suitable model for characterizing photovoltaic devices", Renewable Energy, Vol. 25, pp. 371–380, 2001.

[18] J.S.R. Jang, C.T. Sun, E. Mizutani, Neuro-fuzzy and Soft Computing: A Computational Approach to Learning and Machine Intelligence, New Jersey, Prentice-Hall, 1997.

[19] C. Carrero, J. Rodriguez, D. Ramirez, C. Platero, "Simple estimation of PV modules loss resistances for low error modeling", Renewable Energy, Vol. 35, pp.1103–1108, 2010.

[20] J. Thongpron, K. Kirtikara, C. Jivicate, "A method for the determination of dynamic resistance of photovoltaic modules under illumination", Solar Energy Materials and Solar Cells, Vol. 90, pp. 3078–3084, 2006.

[21] E. Radziemska, "Dark I-U-T measurements of single crystalline silicon solar cells", Energy Conversion and Management, Vol. 46, pp. 1485–1494, 2005.

[22] M. Zagrouba, A. Sellami, M. Bouaicha, M. Ksouri, "Identification of PV solar cells and modules parameters using the genetic algorithms: application to maximum power extraction", Solar Energy, Vol. 84, pp. 860–866, 2010.

[23] A.A. Kulaksız, "ANFIS-based parameter estimation of one-diode equivalent circuit model of PV modules", IEEE 12th International Symposium on Computational Intelligence and Informatics, pp. 415–420, 2011.

[24] D.L. King, Sandia's PV Module Electrical Performance Model, 2000.

[25] D.L. King, "Photovoltaic module and array performance characterization methods for all system operating conditions", Proceedings of the NREL/SNL Photovoltaics Program Review Meeting, pp. 1–22, 1997.

[26] Shell SP70 Photovoltaic Solar Module Product Information Sheet. Available at: http://telemetryhelp.com/Datasheets/ShellSP70_USv1.pdf, access date: 29.05.2012.

[27] KC60 High Efficiency Multicrystal Photovoltaic Module Datasheet Kyocera. Available at: <http://www.kyocerasolar.eu/index/products/download/English.-cps-33141-files-40356-File.cpsdownload.tmp/DB-E-KC60.pdf>, access date: 29.05.2012.

[28] Shell S75 Photovoltaic Solar Module Product Information Sheet. Available at: <www.solarcellsales.com/techinfo/docs/ShellSolarS75_UKv5.pdf>, access date: 29.05.2012.

[29] Shell ST40 Photovoltaic Solar Module Product Information Sheet. Available at: <http://telemetryhelp.com/Datasheets/ShellST40_USv1.pdf>, access date: 29.05.2012.

[30] D.S.H. Chan, J.C.H. Phang, "Analytical methods for the extraction of solar-cell single- and double-diode model parameters from I–V characteristics", IEEE Transactions on Electron Devices, Vol. ED-34, pp. 286–293, 1987.

[31] T. Easwarakhanthan, J. Bottin, I. Bouhouch, C. Boutrit, "Nonlinear minimization algorithm for determining the solar cell parameters with microcomputers", International Journal of Solar Energy, Vol. 4, pp. 1–12, 1986.

[32] PSIM software, Available at: <http://www.psim-europe.com>, access date: 29.05.2012.